CHEMICAL ENGINEERING TRANSACTIONS
VOL. 119, 2025
A publication of AIDIC
The Italian Association of Chemical Engineering
Online at www.cetjournal.it
Guest Editors: David Bogle, Flavio Manenti, Piero Salatino

ISBN 979-12-81206-20-5; **ISSN** 2283-9216
DOI: 10.3303/CET25119089

Chemical Profiling of RI6 Durian Peel (*Durio zibethinus* Murr.) and Lignin Characterization

Anh P.T. Nguyen[a,b], Phuc H. Kha[a,b], Luong T. Ly[a], Khoa D.N. Vo[a], Thuy T.T Nguyen[a,*]

[a]Institute of Advanced Technology (IAT), Vietnam Academy of Science and Technology (VAST), Ho Chi Minh City 700000, Vietnam
[b]Graduate University of Science and Technology (GUST), Vietnam Academy of Science and Technology (VAST), Hanoi 100000, Vietnam
thanhthuy@iat.vast.vn

Durian peel, which accounts for up to 70 % of its fruit weight and is often discarded as waste, has been emerging as a valuable source of bio-compounds, including cellulose, lignin, pectin, and other natural substances. In order to valorize these components, the research successfully exploited the chemical composition of Ri6 durian rind powder, such as ethanol extract, pectin, and α-cellulose with respective contents of 12.85 %, 9.08 %, and 28.19 %. Notably, lignin was first extracted from durian peel using two methods: Kraft and alkaline pulpings, with yields of 13.21 % and 7.96 %, respectively. Comprehensive characterization of the extracted compounds was performed using nuclear magnetic resonance (NMR), Fourier-transform infrared spectroscopy (FT-IR), energy dispersive X-ray spectroscopy (EDX), and X-ray diffraction (XRD). This study highlights the potential of durian peels as a sustainable source of functional ingredients and natural additives, contributing to waste recycling and circular economy efforts.

1. Introduction

The growing global demand for sustainable, bio-based materials has intensified research into plan-derived compounds for diverse industrial applications. As the world moves towards greener alternatives, fruit rinds have attracted significant attention due to their potential as rich sources of bioactive compounds, which exhibit advantageous bioactivities, including antioxidant, antimicrobial, anti-inflammatory properties and demonstrate considerable potential for applications across cosmetic industries, pharmaceuticals, and food (Hussain et al., 2022).Durian, a fruit tree widely grown in Southeast Asia, is a specialty that brings economic benefits to many countries, including Vietnam, Thailand, Philippines, Malaysia, etc. Ri6 durian (*Durio zibethinus* Murr.) is the most popular cultivated variety owing to its good growth potential, large fruits, beautiful thick and dark yellow flesh, flat seeds, strong aroma and englamour taste. However, like other durians, the flesh of the Ri6 variety constitutes only about 20-35 % of the fruit's total weight, the seeds account for 5–15 %, and the remaining 60–75 % is the discarded fruit peel. Therefore, the amount of agro-waste generated from durian peels each year is tremendous. In addition, durian rinds are thick and quite hard; their complex structural fibers bio-decompose more slowly than other biomass lignocelluloses, so burning or burying them will not be an optimal solution. Moreover, the burning process of agro by-products discharges enduring particle matters (PM2.5, PM10); thus, improper treatments of these wastes for a long time have caused a severe impact on the environment. Currently, a number of researches have been conducted using durian peel as raw material, for instance, producing organic fertilizer as biochar, using durian peel fiber as a reinforced filler in composite biomaterials (Chua et al., 2023).
Despite their abundance and potential, durian peels need to be more utilized in both scientific research and industrial processing. The valorization of durian peels is in line with the principles of the circular economy, which advocates for the efficient utilization of resources and waste minimization. The efficient reuse of this agricultural biomass not only elevates economic profits but also contributes to protecting the environment in the long term. Until now, existing studies on durian peel have only focused on the extraction of individual components; there

Paper Received: 10 June 2025; Revised: 3 July 2025; Accepted: 24 September 2025
Please cite this article as: Nguyen A.P., Kha P.H., Ly L.T., Vo K.D., Nguyen T.T., 2025, Chemical Profiling of RI6 Durian Peel (Durio zibethinus Murr.) and Lignin Characterization, Chemical Engineering Transactions, 119, 529-534 DOI:10.3303/CET25119089

is no detailed research on its complete chemical composition, especially lignin. Besides, an appropriate procedure to thoroughly resolve the durian agro-waste is urgently required. Thus, the scope of this work is to preliminarily assess the overall chemical composition, mainly extract, and characterize lignin in Ri6 durian rind. These outcomes will enhance the knowledge on durian peel by-products and their potential applications across various industrial sectors, fostering both sustainability and innovation in the recycling of natural resources.

2. Materials and Methods

2.1 General Chemicals

Quercetin was provided by the Institute of Drug Quality Control (Ho Chi Minh city). Folin-Ciocalteau reagent and pyridine (≥99.0 %) were purchased from Merck (Darmstadt, Germany). Acid gallic (99 %) from Biobasic (Canada). CO_2 was supplied by Vietnguyengas. All other chemical reagents were used as received.

2.2 Durian peel sampling

After collection, 2 kg of Ri6 durian peels were thoroughly washed with water, then sliced into thin sections (5 mm) and dried at 60 ºC to constant weight. The dried durian peel was ground and sieved to collect the fiber with sizes in the range of 300-400 µm. The resulting powder was stored in a desiccator and the moisture content was proceeded by heating in the oven at 60 ºC for 24h .

2.3 Chemical profiling

The process of extracting solvent soluble compounds was carried out by maceration; durian peel powder was soaked in 99.5 % ethanol at a solid-liquid ratio of 1:10 (w/v). After 24 h, the liquid was filtered, this step was repeated three times. The ethanolic filtrate was evaporated to remove the solvent, and subsequently tested for total phenolic and total flavonoid contents using gallic acid and quercetin as standards (Martínez et al., 2022).

$$\% \text{ Ethanolic Extract} = \frac{m_{extraction}}{m_{material}} \times 100\ \% \quad (1)$$

Pectin from durian peel was extracted according to the method of Jong et al. (2023).

$$\% \text{ Pectin} = \frac{m_{pectin}}{m_{material}} \times 100\ \% \quad (2)$$

The determination of total lignin content was performed using the method reported by Tawakkal et al. (2012).

$$\% \text{ Holocellulose} = \frac{m_{material-mass\ loss}}{m_{material}} \times 100\ \% \quad (3)$$

$$\% \text{ Total Lignin} = \frac{\text{Mass loss}}{m_{material}} \times 100\ (\%) \quad (4)$$

Afterwards, hemicellulose was removed from the attained holocellulose using the Kraft process (Jardim et al., 2022).

$$\alpha\text{-cellulose} = \frac{m_{\alpha-cellulose}}{m_{material}} \times 100\% \quad (5)$$

$$\text{Hemicellulose} = \%\ \text{holocellulose} - \%\ \alpha\text{-cellulose} \quad (6)$$

2.4 Extraction of lignin from pectin-free fibers

The Kraft procedure follows the above section, except for the bleaching step with H_2O_2. Alkaline pulping was carried out using the same process, except the white liquor was replaced with a 20 % NaOH solution. Lignin in black liquor from Kraft and alkaline pulpings was precipitated according to previous reports (Al Arni, 2018, Jardim et al., 2022) with slight modifications. Firstly, the black liquor was aerated with pure CO_2 until pH 9, and 50 % H_2SO_4 solution was used to adjust to pH 2. Next, the suspension was heated at 70 ºC for 1 h, cooled to room temperature. Lignin was precipitated by centrifugation at a speed of 10,000 rpm for 10 minutes, neutralized with DI water until pH 7, and freeze-dried.

$$\text{Recovered lignin} = \frac{m_{\text{recovered lignin}}}{m_{material}} \times 100\% \quad (8)$$

$$\text{Lignin recovery yield} = \frac{\%\text{Recovered lignin}}{\%\text{Total lignin}} \times 100\% \quad (9)$$

2.5 Analytical methods

The ash content was determined by heating the samples (1.0 g) in a furnace at 400 °C for 1h.

$$\text{Ash content (\%)} = \frac{\text{weight of ash}}{\text{weight of sample}} \times 100 \quad (10)$$

The functional groups in cellulose and lignin structures were analysed by Fourier transform infrared spectroscopy (FTIR) using a MIR/NIR Frontier spectrometer (PerkinElmer, USA). Data deconvolution was operated via Origin software with a Gaussian peak base on the Levenberg-Marquardt algorithm.

X-ray diffraction (XRD) was carried out using a Panalytical Empyrean diffractometer with Cu-K_α radiation. The crystallinity index (CrI) of cellulose was calculated using the eq. (11) (Pratiwi et al., 2023).

$$\text{CrI (\%)} = \frac{I_{200} - I_{am}}{I_{200}} \times 100 \quad (11)$$

- I_{200}: The maximum intensity of the diffraction peak of the crystal lattice (200) approximately at 2θ from 22° to 23°.
- I_{am}: The maximum intensity of the diffraction peak of the amorphous region located at 2θ from 18° to 19°.

The surficial elemental composition of isolated lignins was analyzed through energy dispersive X-ray spectroscopy (EDX). Elemental analysis was performed on moisture-free Kraft lignin (KL) and alkaline lignin (AL) samples: Total organic carbon was determined using the Walkley–Black method; total nitrogen was measured using the modified Kejldahl method; total sulfur content was assessed using the gravimetric method and the combustion method was used to evaluate total hydrogen. The oxygen content was calculated as 100 − (C + H + N + S + ash).

The ^{1}H-NMR (in $CDCl_3$) analysis was conducted using an Avance III™ HD 500 MHz spectrometer (Bruker Biospin, Switzerland). Acetylated lignin samples were prepared using the process described by Mun et al. (2021).

3. Results and discussion

After the pretreatment, the durian rind powder exhibited a light-yellow color and uniform particle size with a moisture content stabilized at approximately 5.0 % when stored in a sealed jar at room temperature.

3.1 Chemical profiling

The extraction yield by the maceration of durian peel powder in ethanol is 12.85 %. The ethanolic extract comprises a total polyphenols content of 26 mgGAE/g and a total flavonoid content of 16 mgQE/g. This result proves that the ethanol extract from durian rind is not a source of bioactive compounds.

The pectin portion in Ri6 durian peel powder is 9.06 %. Specifically, pectin derived from durian peel demonstrate functional properties that make it suitable for use as a stabilizer, positioning it as a valuable ingredient in various industrial applications and durian rind can serve as a pectin source for commercial product.

The contents of lignin, holocellulose, α-cellulose and hemicellulose are 17.19 %, 48.09, 28.19 and 19.90 %, respectively. In comparison to other fruit peels, durian peel can be considered a rich source of α-cellulose, similar to wood (Lee et al., 2018).

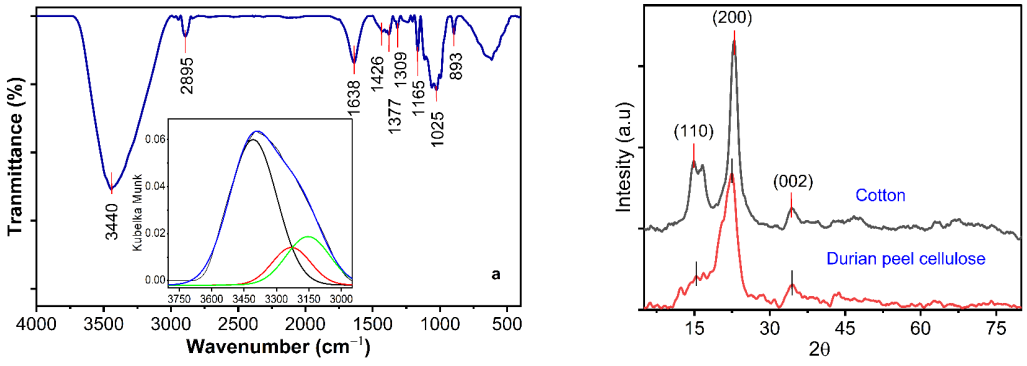

***Figure 1**. FTIR spectrum of α-cellulose from Ri6 durian peel and deconvolution peaks for OH stretching region (a), XRD patterns of α-cellulose from Ri6 durian peel and commercial cotton (b)*

The FTIR spectrum of α-cellulose from durian rind (Figure 1a) exhibits the distinctive peak of the -OH groups at 3440 cm^{-1} and the C–H stretching in CH, CH_2 groups appears at 2895 cm^{-1}. However, no signal was found in the region around 1750 cm^{-1}, which is characteristic of the C=O bond of carbonyl in ester groups in hemicellulose; this result indicates the high purity of α-cellulose product. Furthermore, the infrared spectrum also shows absorption at 1165 and 1025 cm^{-1}, characteristic of C–O–C vibration in the β-(1,4)-glycoside bond of the polysaccharide. Particularly, the absorption peak at 893 cm^{-1} corresponds to the vibration of the glycosidic C–H in the cellulose structure (Boukir et al., 2019). In addition, the deconvolution of the OH vibration band gives more specific information about the inter and intramolecular hydrogen bond in the crystalline region of cellulose

(Kondo, 1997). Apparently, the intramolecular bonding region at 3470 cm^{-1} is the largest peak; while the two smaller intermolecular peaks at 3214 cm^{-1} and at 3314 cm^{-1} are almost equal in intensity. It is evident that intramolecular bonding accounts for the majority of the crystal structure of cellulose, creating its rigidity and stability even being severely affected by chemicals or high-dose irradiation (Driscoll et al., 2009).
The XRD diffractogram of α-cellulose (Figure 1b) gives characteristic diffraction peaks at 2θ = 16.68°, 22.36° and 34.66°, respectively, corresponding to the (110), (200), and (002) lattices, consistent with XRD patterns of commercial cotton. The CrI of the obtained α-cellulose was calculated at 78.6 %, slightly higher than that of commercial cellulose (75.52 %) (Liu et al., 2015). In the study of Pratiwi et al. (2023), lignin was removed by a mixture of $NaClO_2$ and CH_3COOH, then treated with a solution of $(NH_4)_2S_2O_8$, nanocrystalline cellulose was attained with a CrI of 81.62 %. As stated by Lubis et al. (2020), the CrI of durian α-cellulose treated with HNO_3, NaOH, $NaClO_2$, and bleached with H_2O_2 is 60.68 %. Therefore, the hemicellulose removal reagents play a pivotal role in the crystallinity index of the final product. The FTIR and XRD analysis confirm that α-cellulose was successfully separated from Ri 6 durian peel at high purity (99.91 %) with a yield of 28.19 % and a crystallinity index of 78.6 %. The high quality of durian α-cellulose leads to its enhanced functionality in various promising applications.

3.2 Lignin extraction

As reported by Jardim et al. (2022), from 100 g of wood chips, the lignin recovery efficiency from the Kraft pulping was between 66 and 81 %, depending on the type of woods. According to empirical results, after the Kraft process, the lignin in durian peel recovered at 76.85 %, which is in accordance with the published values. The lignin recovery yield from the alkaline process is much lower than from Kraft pulping (46.30 %), confirming that the mixture of NaOH and Na_2S has a better lignin dissolution ability than the sole NaOH solution. However, a small amount of sulfur was introduced into the structure of KL, this is illustrated by EDX elemental analysis (Figure 2b,c) (Akpan and Adeosun, 2019).

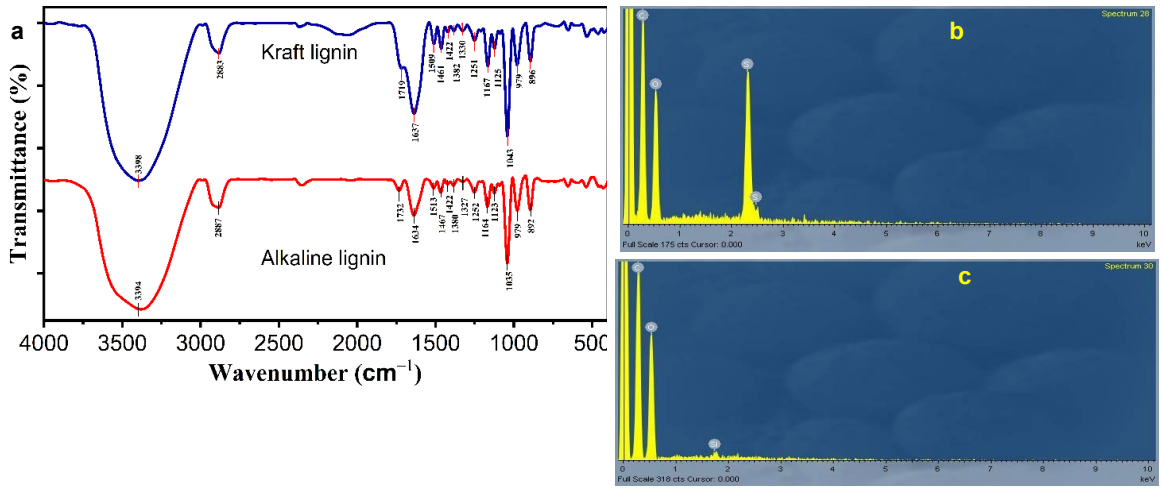

***Figure 2**. FTIR spectra of Kraft and alkaline lignins extracted from Ri6 durian peel (a), EDX elemental analysis of Kraft lignin (b) and alkaline lignin (c)*

FTIR spectra of the two lignins (Figure 2a) display the appearance of a broad peak at 3400 cm^{-1}, representing the OH group of the polyphenol. The absorbances at 2887 and 1383 cm^{-1} indicate the C–H bonds in the methyl and methylene groups. The peaks found at 1637, 1509, 1461, and 1422 cm^{-1} are assigned to the characteristic vibrations of the lignin aromatic ring. The signals at 1328, 1251, and 1044 cm^{-1} exhibit the C–O vibration of G and S units. The additional peaks at 1165 cm^{-1} and 1125 cm^{-1} correspond to the C–H bond in G and S lignin. Furthermore, the absorbances at 979 and 896 cm^{-1} represent the vibration of C–H in substituted aromatic rings (Mun et al., 2021). However, the aliphatic thiol absorption was not observed in FTIR spectrum of KL. The C=O in carbonyl groups is observed around 1700 cm^{-1}, which may arise from lignin's degradation during extraction (Martín-Sampedro et al., 2019).

Table 1. *Elemental composition and empirical formula of Kraft and alkaline lignins extracted from Ri6 durian peel.*

Lignin type	Elemental analysis (%)					Ash (%)	Empirical Formula
	C	H	O	N	S		
Kraft lignin	53.81	4.36	36.37	0.24	4.99	0.23	$C_{4.48}H_{4.36}N_{0.017}S_{0.156}O_{2.27}$
Alkaline lignin	58.70	4.80	35.59	0.32	0.48	0.11	$C_{4.89}H_{4.81}N_{0.023}S_{0.015}O_{2.22}$

The elemental composition and empirical formula of the two lignins were tabulated in Table 1. Since the lignin isolation from durian peel underwent a hot acidic treatment step, the ash contents were extremely low at 0.11 % for KL and 0.23 % for AL. In the case of the Kraft and alkaline extraction, the high oxygen content due to oxidative degradation which introduces ketones and carbonyl groups into the lignin structure, was confirmed by the FTIR analysis. As it was aforementioned that the Kraft pulping chemically modified lignin structure, the sulfur content in KL is ten times higher than in AL. Consequently, durian lignins are more likely to participate in cross-linking reactions due to the reactive oxygen groups, making it suitable for applications in bio-based composites. Among non-destructive analytical methods, ^{1}H NMR stands for a fast and indispensable technique to offer crucial insight into lignin's structure. As showed in Figure 3a, the aromatic hydrogen signals appear from 6.50 to 8.0 ppm; these protons are part of the aromatic rings in guaiacyl (G), syringyl (S) units. The peaks from 5.20 to 6.20 ppm are assigned for noncyclic and cyclic benzylic protons, and the signals from 4.00 to 5.20 ppm and from 0.50 to 1.50 ppm represent the oxygenated aliphatic and non-oxygenated aliphatic protons. In particular, the characteristic protons in the –OCH_3 of G and S monolignols appear from 3.50 to 4.00 ppm, which are critical to the structural diversity of lignin. The aromatic and aliphatic acetoxyl protons were observed in the range of 1.97 to 2.50 ppm. Apparently, durian lignin predominantly comprises S units, evidenced by the peak at 6.62 ppm corresponding to aromatic protons of S units in NMR spectra of both lignins; in contrast, a negligible peak at 7.01 ppm, representing aromatic protons in G units, exclusively presents in the NMR spectrum of Kraft lignin (Ahmad et al., 2020). Moreover, the proton spectroscopic results indicate representative linkages in durian lignin matrix including β-β (H_α at 4.72 ppm), β-O-4/α-O-5 (H_α at 5.03 ppm), β-O-4 (H_α at 6.00 ppm) and β-5 (H_α at 5.45 ppm) (Lundquist, 1979) (Figure 3b). Obviously, the β-β linkage rather than β-O-4 takes up the majority in durian lignin framework because of the high β-β coupling of S alcohol tendency in S-rich lignin (Heitner et al., 2016). Besides, the resonance spectra demonstrate the chemical change in KL structure in comparison to AL, not only the monolingol types but also the interunit linkings. Precisely, AL composes barely of S units and oxidized S unit (δ from 7.20 to 7.36 ppm) (Heitner et al., 2016, Anderson et al., 2019), whereas KL contains a trace of G units. Due to the overlap of the protons in H units and oxidized S unit in ^{1}H NMR spectra, the presence of H monolignols cannot be confirmed. With regard to the distribution of interunit linkages, the β-O-4, β-O-4/α-O-5 and β-β linkages present at similar quantity in KL, while the β-O-4 type attributes a faint role in AL structure. Generally, spectroscopic analyses confirm that lignin was efficiently extracted using Kraft and alkaline methods.

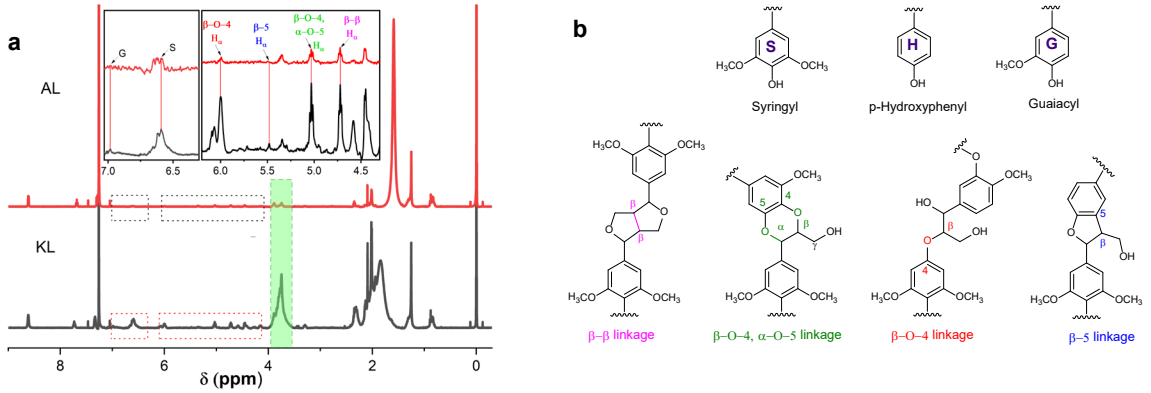

Figure 3*. ^{1}H-NMR spectra of Kraft lignin and alkaline lignin (a), monolignols and representative linkages in durian lignin structure (b)*

4. Conclusion

The chemical components derived from agricultural waste, Ri6 durian peel, were segregated including ethanol extract, pectin, cellulose, and lignin. Significantly, this is the first time that the chemical composition and structure of lignins from Ri6 durian were characterized. Durian lignin consists mostly of syringyl units with β-β, β-O-4/α-

O-5, β-O-4 and β-5 linkings in their structures. The combination of complementary chemical analyses is particularly useful for fundamental studies on lignin. Furthermore, α-cellulose in durian peel was isolated at high purity with a crystallinity index of 78.6 %. This study establishes a foundation for further research aiming at maximizing the potential and enhancing the economic viability of durian peel.

References

Ahmad, Z., W. W. Al Dajani, M. Paleologou and C. Xu, 2020, Sustainable process for the depolymerization/oxidation of softwood and hardwood kraft lignins using hydrogen peroxide under ambient conditions, Molecules, 25, 2329.

Akpan, E. I. and S. O. Adeosun, 2019. Sustainable lignin for carbon fibers: principles, techniques, and applications, Springer.

Al Arni, S., 2018, Extraction and isolation methods for lignin separation from sugarcane bagasse: a review, Industrial Crops and Products ,115, 330-339.

Anderson, E. M., M. L. Stone, R. Katahira, M. Reed, W. Muchero, K. J. Ramirez, G. T. Beckham and Y. Román-Leshkov, 2019, Differences in S/G ratio in natural poplar variants do not predict catalytic depolymerization monomer yields, Nature communications, 10, 2033.

Boukir, A., S. Fellak and P. Doumenq, 2019, Structural characterization of Argania spinosa Moroccan wooden artifacts during natural degradation progress using infrared spectroscopy (ATR-FTIR) and X-Ray diffraction (XRD), Heliyon, 5.

Chua, J. Y., K. M. Pen, J. V. Poi, K. M. Ooi and K. F. Yee, 2023, Upcycling of biomass waste from durian industry for green and sustainable applications: An analysis review in the Malaysia context, Energy Nexus, 10, 100203.

Driscoll, M., A. Stipanovic, W. Winter, K. Cheng, M. Manning, J. Spiese, R. A. Galloway and M. R. Cleland, 2009, Electron beam irradiation of cellulose, Radiation Physics and Chemistry, 78, 539-542.

Heitner, C., D. Dimmel and J. Schmidt, 2016. Lignin and lignans: advances in chemistry, CRC press.

Hussain, H., N. Z. Mamadalieva, A. Hussain, U. Hassan, A. Rabnawaz, I. Ahmed and I. R. Green, 2022, Fruit peels: Food waste as a valuable source of bioactive natural products for drug discovery, Current issues in molecular biology, 44, 1960-1994.

Jardim, J. M., P. W. Hart, L. A. Lucia, H. Jameel and H.-m. Chang, 2022, The effect of the kraft pulping process, wood species, and pH on lignin recovery from black liquor, Fibers, 10, 16.

Jong, S. H., N. Abdullah and N. Muhammad, 2023, Optimization of low-methoxyl pectin extraction from durian rinds and its physicochemical characterization, Carbohydrate Polymer Technologies and Applications, 5, 100263.

Kondo, T., 1997, The assignment of IR absorption bands due to free hydroxyl groups in cellulose, Cellulose, 4, 281-292.

Lee, M. C., S. C. Koay, M. Y. Chan, M. M. Pang, P. M. Chou and K. Y. Tsai, 2018, Preparation and characterization of durian husk fiber filled polylactic acid biocomposites, MATEC Web of Conferences, EDP Sciences.

Liu, Y., J. Chen, X. Wu, K. Wang, X. Su, L. Chen, H. Zhou and X. Xiong, 2015, Insights into the effects of γ-irradiation on the microstructure, thermal stability and irradiation-derived degradation components of microcrystalline cellulose (MCC), RSC Advances, 5, 34353-34363.

Lubis, R., B. Wirjosentono, Eddiyanto and A. A. Septevani, 2020, Preparation and characterization of cellulose pulp from fiber of durian peel.

Lundquist, K., 1979, NMR Studies of Lignine. 2. Interpretation of the Щ NMR Spectrum of Acetylated Birch Lignin, Acta Chemica Scandinavia B, 33, 27-30.

Martín-Sampedro, R., J. I. Santos, Ú. Fillat, B. Wicklein, M. E. Eugenio and D. Ibarra, 2019, Characterization of lignins from Populus alba L. generated as by-products in different transformation processes: Kraft pulping, organosolv and acid hydrolysis, International journal of biological macromolecules, 126, 18-29.

Martínez, S., C. Fuentes and J. Carballo, 2022, Antioxidant activity, total phenolic content and total flavonoid content in sweet chestnut (Castanea sativa Mill.) cultivars grown in Northwest Spain under different environmental conditions, Foods, 11, 3519.

Mun, J.-S., J. A. Pe III and S.-P. Mun, 2021, Chemical characterization of kraft lignin prepared from mixed hardwoods, Molecules, 26, 4861.

Pratiwi, H., Kusmono and M. W. Wildan, 2023, Oxidized cellulose nanocrystals from durian peel waste by ammonium persulfate oxidation, ACS omega, 8, 30262-30272.

Tawakkal, I. S., R. A. Talib, K. Abdan and C. N. Ling, 2012, Mechanical and physical properties of kenaf-derived cellulose (KDC)-filled polylactic acid (PLA) composites, BioResources, 7.